ChemComm

Supramolecular optimization of the visual contrast for colorimetric indicator assays that release resorufin dye

Journal:	*ChemComm*
Manuscript ID	CC-COM-05-2020-003551.R1
Article Type:	Communication

COMMUNICATION

Supramolecular optimization of the visual contrast for colorimetric indicator assays that release resorufin dye†

Received 00th January 20xx,
Accepted 00th January 20xx

DOI: 10.1039/x0xx00000x

Janeala J. Morsby, [a] Madushani Dharmarwardana, [a] Hannah McGarraugh, [a] and Bradley D. Smith [a]*

A tetralactam macrocycle acts as a novel supramolecular adjuvant to capture a released resorufin dye and create a higher contrasting yellow/blue color change for enhanced naked eye interpretation of a colorimetric indicator assay.

There is a growing demand for robust diagnostic technologies that allow point-of-care medical treatment or environmental monitoring to be conducted without electrical power. Technologies that meet the criteria of affordable, sensitive, specific, user-friendly, rapid and robust, equipment free and deliverable (ASSURED) are a high priority.[1,2] Many diagnostic assays have been designed to produce a change in a sample's absorption and/or fluorescence spectrum.[3,4] While fluorescence assays are inherently more sensitive than colorimetric, they require a powered excitation source which is a practical limitation. In contrast, colorimetric indicator assays, especially those based on test strip technology, do not need external power if the results can be detected using the naked eye. The low sensitivity of a colorimetric assay can be circumvented if the chemical event that produces the color change is a catalytic reaction. For example, many enzyme assays utilize an enzyme substrate whose chemical structure releases a colored dye after enzyme action.[3] Similarly, many chemical indicators are reactive molecules that release a colored dye when they are cleaved catalytically by a specific analyte.[4] In these cases, the color change that is caused by the dye release is a detectable signal that is amplified by catalyst turnover.

The ideal colorimetric indicator assay is a signal transduction process that induces a colorless sample to become intensely colored and in this case the assay performance is governed by standard optical parameters such as molar absorptivity of the released dye, color stability, color perception of the human eye, and color homogeneity if the sample is immobilized on a solid phase.[5] In practice, most colorimetric indicators transduce a change between two colors (two-color colorimetric assay). In this case, the assay development process should also aim to optimize the contrast of the "before" and "after" colors for easier perception by the eye.‡

Inspection of the color wheel in Scheme 1 provides systematic guidance for contrast optimization in a two-color colorimetric assay. Colors that are opposite each other on the color wheel are complementary colors because they produce high visual contrast. *Thus, one important experimental goal for optimizing two-color contrast for naked eye interpretation of a colorimetric indicator assay is to ensure that the "before" and "after" colors are complementary colors.*[6] In principle, one way to pursue this goal is to modify the substrate structure by chemical synthesis. However, this approach is time consuming because it requires an iterative cycle of modified substrate synthesis and testing to determine if there is an improvement in color contrast while maintaining appropriate reactivity. Here, we describe a novel alternative approach; that is, a supramolecular strategy that adds a host molecule to the assay solution to bind the released dye and enhance the visual contrast for naked eye detection.

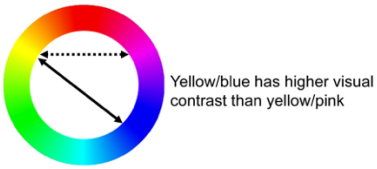

Scheme 1. Colors that are opposite on the color wheel are complementary and produce the highest visual contrast.

Many fluorescent dyes undergo a substantial change in brightness when captured by a supramolecular host, and various host molecules have been studied extensively as adjuvants to enhance the performance of fluorescent chemosensor or enzyme assays.[7] In contrast, there are very few examples of colored dyes that strongly change absorption profile upon supramolecular capture.[7,8] The focus here is on colorimetric indicators that release the well-known phenoxazine dye, resorufin (**RF**) whose structure is shown in Scheme 2. There are several dozen publications describing a wide range of different enzyme substrates and reactive chemosensors that release **RF** (see ESI Table S1 for a summary).[3,4,9–14] These yellow-colored compounds are weakly fluorescent. The cleavage reaction is highly fluorogenic due to the appearance of pink-colored **RF** which has very bright emission properties, and the vast majority of published studies have focused on fluorescence assays. Some reports have suggested that the sample color change from pink to yellow has value as a colorimetric assay, but as indicated by the color wheel in

[a] *Department of Chemistry and Biochemistry, 251 Nieuwland Science Hall, University of Notre Dame, Notre Dame, IN 46556, USA*
**Email: smith.115@nd.edu*
†Electronic Supplementary Information (ESI) available: Experimental section, synthesis, supplementary figures, modeling data, and references. See DOI: 10.1039/x0xx00000x

Scheme 1, the change is hard to perceive with the naked eye. Unfortunately, this means that the large collection of known **RF**-releasing chemosensors and substrates is currently not very useful for colorimetric analysis. Thus, the general project goal was to find a suitable supramolecular host that could enhance the two-color contrast of a **RF**-releasing indicator assay.

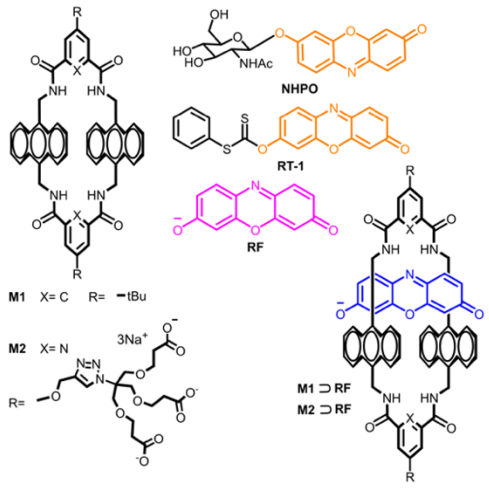

Scheme 2. Chemical structures.

The choice of a supramolecular host for released **RF** was based on our previous experience with tetralactam macrocycles containing aromatic sidewalls, which are versatile synthetic receptors for a wide range of guest molecules.[15] They are especially effective as supramolecular hosts for squaraine dyes where dye complexation produces a noticeable red shift in dye absorption.[16,17] Recent work by Mateo-Alonso and co-workers has shown that tetralactam macrocycles with anthracene sidewalls can capture acene guests by a combination of guest hydrogen bonding with the internally directed macrocycle NH residues and aromatic stacking with anthracene sidewalls.[18] With this knowledge in mind, we wondered if tetralactam macrocycles could be used to capture **RF** and enhance the effectiveness of **RF**-releasing substrates and chemosensors in colorimetric assays. Here, we report **RF** complexation studies using the organic and water soluble tetralactam hosts, **M1** and **M2**, and our finding that **RF** encapsulation induces a remarkable red-shift effect that produces a highly desired blue colored complex. In addition, we show that supramolecular **RF** encapsulation can change the before/after colors of a two-color colorimetric assay from a yellow/pink pair to a higher contrasting yellow/blue pair which is easier to perceive by the naked eye.

Early experimental evidence that a tetralactam macrocycle can encapsulate **RF** was gained by conducting host/guest association studies in chloroform. Absorption and fluorescence experiments found that addition of organic-soluble macrocycle **M1** to **RF** (tetrabutylammonium salt) induced a red-shift in **RF** absorption maxima band and quenching of **RF** fluorescence (Figure S5). ^{1}H NMR titration experiments in $CDCl_3$ produced spectra exhibiting exchange-induced line broadening, a common occurrence in host/chemistry (Figure S4),[19] but there was still strong proof that the **RF** was encapsulated inside **M1**. The spectral comparison in Figure 1 highlights the complexation-induced changes in macrocycle chemical shift upon formation of **M1⊃RF**. The large down-field changes in chemical shift for macrocycle NH residues and internally directed protons B are strong indicators of hydrogen bonding with **RF** heteroatoms.

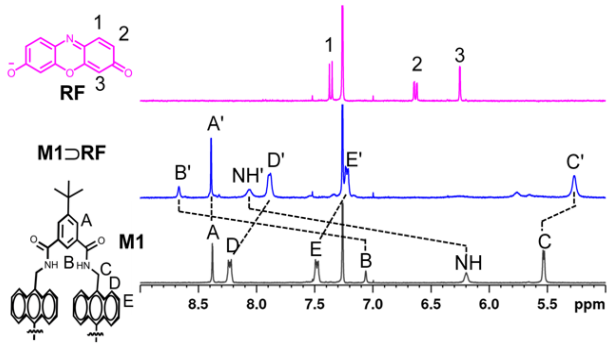

Figure 1. Partial ^{1}H NMR spectra (500 MHz, $CDCl_3$, 25° C) of: *(top)* **RF** (0.5 mM), *(center)* **M1⊃RF** (0.5 mM), and *(bottom)* **M1** (0.5 mM). For clarity, the tetrabutylammonium cation peaks are not shown

Shown in Figure 2 is a molecular model that is highly consistent with the spectral data and the previous literature on acene encapsulation within macrocycles like **M1**.[15,18] The modeling indicates that the macrocycle NH residues form bifurcated hydrogen bonds with the internal oxygen and nitrogen atoms on the anionic **RF** guest which is consistent with literature computations showing that these atoms are reasonable hydrogen bond acceptors.[20,21] **RF** encapsulation is also favored by the large amount of aromatic surface area that is engaged in favorable π-π stacking interactions.

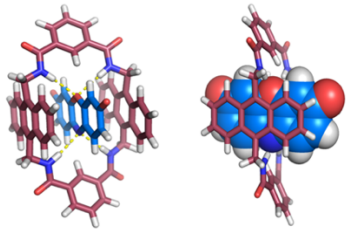

Figure 2: Two views of a molecular model of **M1⊃RF** (macrocycle lacks t-butyl groups) that was computed using the PM7 method.

RF complexation studies in water used the known tetralactam macrocycle **M2**, with two appended dendritic tricarboxylates as water solubilizing units.[22,23] Absorption and fluorescence experiments found that addition of water-soluble macrocycle **M2** to **RF** created a blue colored complex with absorption maxima band at 624 nm (Figure 3a). In addition, there was substantial complexation-induced quenching of **RF** fluorescence which enabled fluorescence titration experiments. Shown in Figure 3b is a representative fluorescence titration curve that was fitted, using a standard non-linear computer algorithm, to a 1:1 binding model. The average of three independent experiments determined K_a to be $(3.2 \pm 0.6) \times 10^5$ M^{-1} which is more than 100 times higher than the **RF** affinity reported for β-cyclodextrin.[24] Control experiments that acquired the absorption profile of **RF** in different solvents showed that the absorption maxima band is weakly red-shifted by a change from water to aprotic organic solvent (Figures 3a and S3). But in no solvent is the absorption maxima wavelength higher than 600 nm. Similarly, **RF** absorption is still below 600 nm when it is encapsulated within micelles or β-cyclodextrin.[24,25,26] Thus, the remarkably large complexation-induced red-shift of **RF** absorption maxima wavelength to 624 nm is not simply due to a less polar

microenvironment inside the cavity of **M2**. More likely, intermolecular π-π interactions between the encapsulated **RF** and the anthracene sidewalls of **M2** induces a Davydov splitting effect that lowers the **RF** excited state energy,[27,28] and also promotes quenching of **RF** fluorescence by photoinduced electron transfer.[29]

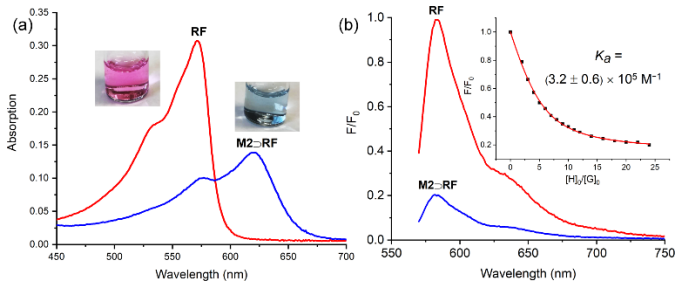

Figure 3. (a) Partial absorption (a) and emission (ex: 540 nm) (b) spectra in water (25°C) of 10 μM **RF** (sodium salt) (red line) and 10 μM **M2**⊃**RF** (blue line), with the latter obtained by mixing 10 μM **RF** and 200 μM **M2**. Insert: representative titration isotherm showing decrease in fluorescence (ex: 540 nm, em: 585 nm) for **RF** (10 μM) with increasing equivalents of **M2** in water, red line shows curve fitting to a 1:1 binding model.

To demonstrate potential utility as a colorimetric indicator, we investigated two diagnostic applications that are relevant to the ongoing coronavirus pandemic. The first study examined the effect of **M2** on the colorimetric performance of **RT-1** (Scheme 1), a known **RF**-releasing chemosensor for fluorescence detection of hypochlorous acid.[30] We reasoned that **RT-1** could be repurposed as a colorimetric indicator of hypochlorite (denoted here as HOCl/OCl$^-$ since the pKa is 7.5), a reactive chemical that is employed world-wide as a bleaching agent or as a common disinfectant. A manifestation of the COVID-19 pandemic is increased environmental exposure to water samples containing HOCl/OCl$^-$. Thus, effective indicator tests are needed to rapidly determine if water samples contain HOCl/OCl$^-$ which can cause health problems such as skin irritation or inflammation of the esophagus. In addition, there is a need to know if a procured disinfectant solution is sufficiently concentrated for useful operation. The literature includes several recent reports of chemosensor candidates for colorimetric HOCl/OCl$^-$ detection.[31–37] Operationally, **RT-1** is an attractive choice as an indicator of HOCl/OCl$^-$ because it is chemically quite selective, the cleavage reaction is complete within a few minutes, and there is a linear relationship in the low micromolar range between concentration of HOCl/OCl$^-$ and released **RF**.[30] As shown in Figure 4, addition of HOCl/OCl$^-$ (5 μM) induces rapid chemical fragmentation of yellow **RT-1** to produce a pink solution due to the released **RF**. Subsequent addition of macrocycle **M2** to the sample instantly produces a blue color due to the formation of **M2**⊃**RF**. Thus, addition of **M2** enhances the performance of **RT-1** as a two-color indicator of HOCl/OCl$^-$ by converting the yellow/pink color change to a yellow/blue color change that is more easily perceived by the naked eye. A second proof of concept study assessed the potential of **M2** to enhance an enzyme assay that released **RF**. We chose **NHPO** as a known substrate for the enzyme *N*-Acetyl-β-*D*-glucosaminidase (NAG) which is a clinically relevant urinary biomarker of kidney dysfunction.[3] A relatively high level of NAG in the urine is thought to reflect chronic kidney disease in disorders such as diabetes,[38] and may indicate acute kidney injury in patients with severe COVID-19.[39]

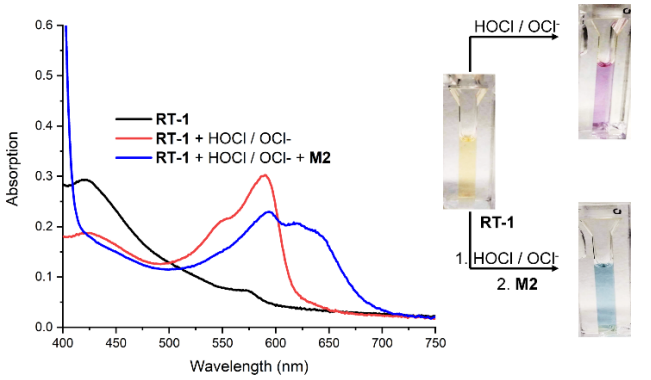

Figure 4. Absorbance spectra and photographs of a sample, initially containing **RT-1** (50 μM, black line), and 3 minutes after addition of HOCl/OCl$^-$ (5 μM, red line), or 3 minutes after a two-step addition sequence of HOCl/OCl$^-$ (5 μM) and then **M2** (500 μM) (blue line). In 200 mM PBS, pH 7.4 at 25°C.

Thus, there is a need for simple and robust urinalysis tests that allow a patient to identify early stages of kidney dysfunction or track kidney health during treatment. Recently, **NHPO** probe was shown to be an effective fluorescent substrate for NAG;[3] thus, our goal was to ascertain if macrocycle **M2** could enhance the performance of **NHPO** as a colorimetric indicator of NAG enzyme. As shown in Figure 5, addition of NAG leads to enzyme catalysed fragmentation of yellow **NHPO** to produce a pink solution of **RF**. Adding an aliquot of **M2** to the assay solution leads to a deep-purple color due to complexation of the released **RF** by the **M2**. The assay mixture included BSA as an enzyme stabilizer which competes for the **RF**,[40] and slightly weakens the supramolecular color enhancement effect (there is no evidence for NAG or BSA interaction with **M2**, Figure S9). Nonetheless, the presence of **M2** still converts the before/after colors of the colorimetric NAG assay using **NHPO** from yellow/pink to yellow/deep-purple, a color change that is more easily perceived by the naked eye.

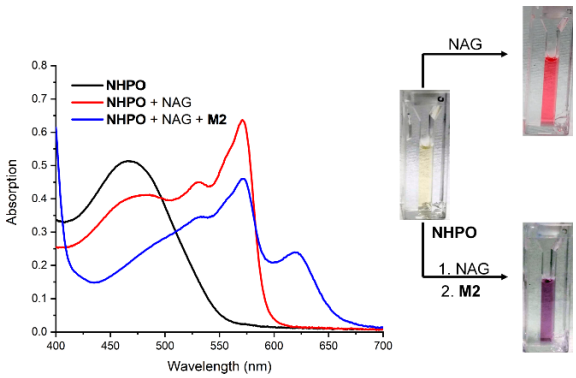

Figure 5. Absorbance spectra and photographs of a sample, initially containing **NHPO** (50 μM), and 30 minutes after addition of NAG enzyme (0.9 μg/mL), red line), or 45 minutes after a two-step addition of NAG (0.9 μg/mL) and **M2** (500 μM) (blue line). In 100 mM PBS + 100 μM BSA pH 7.4 at 25°C.

In summary, the vast majority of known colorimetric chemical indicators and enzyme substrates are "two-color" assays. Thus, indicator development projects should aim to design the "before" and "after" colors to be complementary colors because they produce the highest visual contrast for naked eye perception (Scheme 1).[6] **RF**-releasing chemosensors and enzyme substrates are ubiquitous but unfortunately the inherent yellow/pink color change is not very

useful for colorimetric detection by the naked eye. We find that tetralactam **M2** can be employed as a supramolecular adjuvant to capture the released **RF** and create a higher contrasting yellow/blue color change. This simple assay modification should be broadly useful because there are several dozens of different enzyme substrates and reactive chemosensors that release **RF**. From a broader perspective, this study provides proof of concept for a new and potentially generalizable supramolecular chemistry strategy for fine-tuning the visual contrast of two-color indicator assays for naked eye detection. The next step in the research is development of indicator test strips where we will build on our previous success using a surface-immobilized tetralactam host for dye capture.[41] We are grateful for funding support from the NIH (R01GM059078, R35GM136212 and T32GM075762) and NSF (CHE1708240) and we acknowledge D. -H. Li for conducting the molecular modelling.

Conflicts of interest

There are no conflicts to declare.

Notes and references

‡ Color analysis methods that employ externally powered detection devices are outside the scope of this report; however, the interested reader is directed to reference 5.

1 S. Smith, J. G. Korvink, D. Mager and K. Land, *RSC Adv.*, 2018, **8**, 34012–34034.
2 K. J. Land, D. I. Boeras, X.-S. Chen, A. R. Ramsay and R. W. Peeling, *Nat. Microbiol.*, 2019, **4**, 46–54.
3 F. Yan, X. Tian, Z. Luan, L. Feng, X. Ma and T. D. James, *Chem. Commun.*, 2019, **55**, 1955–1958.
4 M. G. Choi, S. Y. Park, K. Y. Park and S. K. Chang, *Sci. Rep.*, 2019, **9**, 1–8.
5 G. Gianini, T. Mazzu-nascimento, A. M. Stockton and E. Carrilho, *Anal. Chim. Acta*, 2017, **970**, 1–22.
6 H. H. Cho, S. H. Kim, J. H. Heo, Y. E. Moon, Y. H. Choi, D. C. Lim, K. H. Han and J. H. Lee, *Analyst*, 2016, **141**, 3890–3897.
7 R. N. Dsouza, U. Pischel and W. M. Nau, *Chem. Rev.*, 2011, **111**, 7941–7980.
8 S. Gupta, Y. Zhao, R. Varadharajan and V. Ramamurthy, *ACS Omega*, 2018, **3**, 5083–5091.
9 T. Yoshiya, H. Ii, S. Tsuda, S. Kageyama, T. Yoshiki and Y. Nishiuchi, *Org. Biomol. Chem.*, 2015, **13**, 3182–3185.
10 S. Y. Kim and J. I. Hong, *Org. Lett.*, 2007, **9**, 3109–3112.
11 J. Wang, Y. Men, L. Niu, Y. Luo, J. Zhang, W. Zhao and J. Wang, *Chem. Asian J.*, 2019, **14**, 3893–3897.
12 E. L. Smith, C. R. Bertozzi and K. E. Beatty, *ChemBioChem*, 2014, **15**, 1101–1105.
13 G. Magro, R. E. S. Bain, C. A. Woodall, R. L. Matthews, S. W. Gundry and A. P. Davis, *Environ. Sci. Technol.*, 2014, **48**, 9624–9631.
14 H. Zhang, C. Xu, J. Liu, X. Li, L. Guo and X. Li, *Chem. Commun.*, 2015, **51**, 7031–7034.
15 D. H. Li and B. D. Smith, *Beilstein J. Org. Chem.*, 2019, **15**, 1086–1095.
16 F. M. Roland, E. M. Peck, D. R. Rice and B. D. Smith, *Bioconjug. Chem.*, 2017, **28**, 1093–1101.
17 T. S. Jarvis and B. D. Smith, *Supramol. Chem.*, 2019, **31**, 140–149.
18 C. Gozalvez, J. L. Zafra, A. Saeki, M. Melle-Franco, J. Casado and A. Mateo-Alonso, *Chem. Sci.*, 2019, **10**, 2743–2749.
19 T. C. S. Pace and C. Bohne, *Adv. Phys. Org. Chem.*, 2007, **42**, 167–223.
20 J. Lv and D. Yang, *Comput. Theor. Chem.*, 2011, **970**, 6–14.
21 D. Yang and Y. Liu, *J. Chin. Chem. Soc.*, 2012, **59**, 967–974.
22 C. F. A. Gómez-Durán, W. Liu, D. Lourdes and B. D. Smith, *J. Org. Chem.*, 2017, **82**, 8334–8341.
23 J. M. Dempsey, C. Zhai, H. H. Mcgarraugh, C. L. Schreiber, S. E. Stoffel and B. D. Smith, *Chem. Commun.*, 2019, **55**, 12793–12796.
24 R. Csepregi, B. Lemli, S. Kunsagi-Mate, L. Szente, T. Koszegi, B. Nemeti and M. Poor, *Molecules*, 2018, **23**, 382.
25 G. V Porcal, C. M. Previtali and S. G. Bertolotti, *Dyes. Pigm.*, 2009, **80**, 206–211.
26 G. V Porcal, M. S. Altamirano, C. A. Glusko, S. G. Bertolotti and C. M. Previtali, *Dyes. Pigm.*, 2011, **88**, 240–246.
27 B. S. Basel, C. Hetzer, J. Zirzlmeier, D. Thiel, R. Guldi, F. Hampel, A. Kahnt, T. Clark, D. M. Guldi and R. R. Tykwinski, *Chem. Sci.*, 2019, **10**, 3854–3863.
28 B. L. Cannon, L. K. Patten, D. L. Kellis, P. H. Davis, J. Lee, E. Graugnard, B. Yurke and W. B. Knowlton, *J. Phys. Chem. A*, 2018, **122**, 2086–2095.
29 A. Montejano, M. Gervaldo and S. G. Bertolotti, *Dyes. Pigm.*, 2005, **64**, 117–124.
30 M. G. Choi, Y. J. Lee, K. M. Lee, K. Y. Park, T. J. Park and S. Chang, *Analyst.*, 2019, **144**, 7263–7269.
31 S. Naha, A. Varalakshmi and S. Velmathi, *Spectrochim. Acta A.*, 2019, **220**, 1–10.
32 Y. Zhang, Z. Wang, S. Hou, H. Wang, X. Zhang and X. Chen, *Analyst*, 2020, **145**, 939–945.
33 A. Manna and S. Goswami, *New J. Chem.*, 2015, **39**, 4424–4429.
34 Y. Guo, Q. Ma, F. Cao, Q. Zhao and X. Ji, *Anal. Methods*, 2015, **7**, 4055–4058.
35 Q. Han, F. Zhou, Y. Wang, H. Feng, Q. Meng, Z. Zhang, and R. Zhang, *Molecules*, 2019, **24**, 2455.
36 H. Pan, Y. Liu, S. Liu, Z. Ou, H. Chen and H. Li, *Talanta*, 2019, **202**, 329–335.
37 L. Wu, Q. Yang, L. Liu, A. C. Sedgwick, A. J. Cresswell, S. D. Bull, C. Huang and T. D. James, *Chem. Commun.*, 2018, **54**, 8522–8525.
38 E. B. Omozee, E. I. Okaka and A. E. Edo, *J. Lab. Physicians*, 2020, **11**, 1–4.
39 D. Batlle, M. J. Soler, M. A. Sparks, S. Hiremath, A. M. South, P. A. Welling and S. Swaminathan, *J. Am. Soc. Nephrol.*, 2020, **31**, 1–4.
40 K. D. Wittrup and J. E. Bailey, *Cytometry*, 1988, **9**, 394–404.
41 W. Liu, C. F. A. Gómez-Durán and B. D. Smith, *J. Am. Chem. Soc.*, 2017, **139**, 6390–6395.

For TOC only

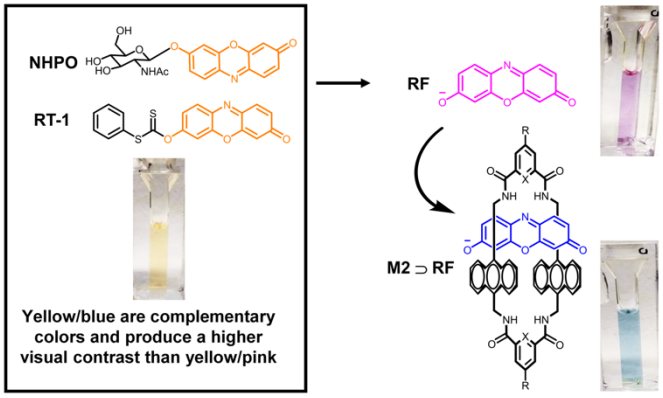

A tetralactam macrocycle captures released resorufin and creates a pair of complementary indicator assay colors that are more easily perceived by the naked eye.